

This discussion paper is/has been under review for the journal Atmospheric Chemistry and Physics (ACP). Please refer to the corresponding final paper in ACP if available.

French airborne lidar measurements for Eyjafjallajökull ash plume survey

P. Chazette et al.

French airborne lidar measurements for Eyjafjallajökull ash plume survey

P. Chazette¹, A. Dabas², J. Sanak¹, M. Lardier³, and P. Royer^{1,3}

¹Laboratoire des Sciences du Climat et de l'Environnement (LSCE), UMR8212, CNRS – Laboratoire mixte CEA-CNRS-UVSQ, CEA Saclay, 91191 Gif-sur-Yvette, France

²Groupe d'Etude de l'Atmosphère Météorologique, URA Météo-France/CNRS, 42 avenue Coriolis, 31100 Toulouse, France

³LEOSPHERE, 76 rue de Monceau, 75008 Paris, France

Received: 28 January 2012 – Accepted: 13 February 2012 – Published: 2 March 2012

Correspondence to: P. Chazette (patrick.chazette@lsce.ipsl.fr)

Published by Copernicus Publications on behalf of the European Geosciences Union.

Title Page

Abstract

Introduction

Conclusions

References

Tables

Figures

⏪

⏩

◀

▶

Back

Close

Full Screen / Esc

Printer-friendly Version

Interactive Discussion

Abstract

An Ultra-Violet Rayleigh-Mie lidar has been integrated aboard the French research aircraft Falcon 20 in order to monitor the ash plume emitted by the Eyjafjallajökul volcano in April–May 2010. Three operational flights were carried out on 21 April, 12 and 16 May 2010 inside French, Spanish and British air spaces, respectively. The original purpose of the flights was to provide the French civil aviation authorities with objective information on the presence and location of the ash plume. The present paper presents the results of detailed analyses elaborated after the volcano crisis. They bear on the structure of the ash clouds and their optical properties such as ash extinction coefficient and lidar ratio. Lidar ratios were measured in the range of 33 to 48 sr, in good agreement with the ratios derived from ground-based lidar measurements performed near Paris (France) in April 2010 (~ 47 sr). The ash signature in terms of particulate depolarization was consistent around $45 \pm 7\%$ during all flights. Such a value seems to be a good identification parameter for ash. Using specific cross-sections between 0.29 and $1.1 \text{ m}^2 \text{ g}^{-1}$, the minimum (maximal) mass concentrations in the ash plumes are derived for the flights on 12 and 16 May. They were 190 (2300) and 270 (1600) $\mu\text{g m}^{-3}$, respectively. It may be rather less than, or of the order of the critical level of damage (2 mg m^{-3}) for the aircraft engines, but well above the $200 \mu\text{g m}^{-3}$ warning level.

1 Introduction

Due to the winds prevailing in Northern Europe at the time, the ash plume emitted by the Icelandic volcano Eyjafjallajökull (e.g. Sigmundsson et al., 2010) that erupted in April–May 2010 was advected from Iceland to the south-east. For several days, it “contaminated” the airspace of Western Europe and lead to a major air traffic disruption (Gertisser, 2010). In France, the “Direction Générale de l’Aviation Civile” (DGAC) and the government authorities closed the airspace entirely from 16 to 21 April 2010, and partially (south-western part of France or Island/UK) from 12 to 16 May 2010.

French airborne lidar measurements for Eyjafjallajökull ash plume survey

P. Chazette et al.

Title Page

Abstract

Introduction

Conclusions

References

Tables

Figures

⏪

⏩

◀

▶

Back

Close

Full Screen / Esc

Printer-friendly Version

Interactive Discussion



During these two periods several lidars were operated by various groups throughout Europe with the purpose of increasing knowledge on ash properties and assess their potential danger to aviation. Ansmann et al. (2011) proposed an original approach coupling lidar and sunphotometer to retrieve the content of ash over central Europe using the existent networks AERONET and EARLINET. The coupling between ground-based remote sensors including lidar was also proposed by Gasteiger et al. (2011) to constrain the ash size distribution. Another original work was conducted by Chazette et al. (2011) using the coupling between lidar (ground-based and spaceborne systems), sunphotometer and modeling to retrieve the ash optical properties over the Paris area and the assessment of the ash mass concentration. The ash plume was also analyzed with active (e.g. Chazette et al., 2011) and passive (e.g. Millington et al., 2012) spaceborne sensors. This last approach followed the work of Prata et al. (2010) and Thomas and Watson (2010) by using multispectral remote-sensing observations from satellites to characterize volcanic emission from space. Following the Eyjafjallajökull eruptions, the airborne measurements played also a major role for the retrieval of microphysical ash properties using sampling approaches (Schumann et al., 2011; Johnson et al., 2012; Bukowiecki et al., 2011) and lidar measurements (e.g. Marengo et al., 2011).

The use of lidar measurements to characterize volcanic aerosols is not new. Following the major eruptions of El Chichon in 1982 and Mount Pinatubo in 1991, volcanic plumes were extensively studied by both ground-based and airborne lidars. For instance, Jäger (1992) used a lidar at Garmisch-Partenkirchen (Germany) to investigate the volcanic aerosol in the stratosphere following the Mount Pinatubo eruption. Simultaneously, lidar measurements were performed at Hampton (Virginia, USA) by Osborn et al. (1995). In France, Chazette et al. (1995) used lidar observations from the “Observatoire de Haute Provence” (OHP) to characterize the aerosol plume in the stratosphere following the eruptions of El Chichon and Mount Pinatubo. The residence time of volcanic aerosols was thus assessed. The ash plume of Mount Pinatubo was also investigated with an airborne lidar by Winker et al. (1992).

French airborne lidar measurements for Eyjafjallajökull ash plume survey

P. Chazette et al.

[Title Page](#)[Abstract](#)[Introduction](#)[Conclusions](#)[References](#)[Tables](#)[Figures](#)[⏪](#)[⏩](#)[◀](#)[▶](#)[Back](#)[Close](#)[Full Screen / Esc](#)[Printer-friendly Version](#)[Interactive Discussion](#)

In this paper we present the contribution of the sole French airborne lidar (AL) that flew during the international airline crisis caused by the Eyjafjallajökul eruption. The AL was built from an ALS450 manufactured by the Leosphere Compagny and initially developed at the “Laboratoire des Sciences du Climat et de l’Environnement” (LSCE).

A similar system has already flown aboard an ultra-light aircraft during the African Monsoon Multidisciplinary Analyses (AMMA) (e.g. Chazette et al., 2007), as well as aboard the FAAM BAe-146 research aircraft (www.faam.ac.uk) (e.g. Marengo et al., 2011). The lidar is briefly presented in Sect. 2 where we also remind how aerosol optical properties can be derived from the co-polar and cross-polar channels of a lidar. The flight plans are presented in Sect. 3 with the identification of the ash plume from the cross-polar channel. In Sect. 4, the ash plume optical properties retrieved from the lidar profiles are presented with their uncertainties and we propose an estimation of the ash mass concentration using the previous results published in the scientific literature. Section 5 summarizes the findings.

2 The airborne lidar

The AL was flown aboard the Falcon 20 (F-20) of the “Service des Avions Français Instrumentés pour la Recherche en Environnement” (SAFIRE, see www.safire.fr) which operates several aircrafts for research purposes in the environment domain. SAFIRE Falcon 20 is an original Dassault Falcon 20 GF specially modified for scientific uses. Its usual cruising speed is 150 m s^{-1} and its endurance is close to 5 h (maximal flight range $\sim 4100 \text{ km}$) depending on the scientific payload (usually $\sim 1200 \text{ kg}$). Its maximum flight ceiling is $\sim 42\,000 \text{ ft}$ ($12\,000 \text{ m}$).

2.1 Technical characteristics of the AL

The AL is a modified version of the ALS450 manufactured by the LEOSPHERE Compagny (www.leosphere.com). It emits in the ultraviolet (355 nm), and is based on a

French airborne lidar measurements for Eyjafjallajökull ash plume survey

P. Chazette et al.

Title Page

Abstract

Introduction

Conclusions

References

Tables

Figures

⏪

⏩

◀

▶

Back

Close

Full Screen / Esc

Printer-friendly Version

Interactive Discussion



20 Hz pulsed Nd:YAG laser (ULTRA) manufactured by QUANTEL (www.quantel.com). Its main characteristics are summarized in Table 1. It was originally jointly developed by LSCE (www.lsce.ipsl.fr) and LEOSPHERE (Chazette et al., 2007; Raut and Chazette, 2009). The UV pulse energy is 16 mJ and the pulse repetition rate is 20 Hz. The receiver implements two channels for the detection of the elastic backscatter from the atmosphere in the parallel and perpendicular polarization planes relative to the linear polarization of the emitted radiation. It was designed to monitor the aerosol distribution and dispersion in the low and middle troposphere. It enables the retrieval of aerosol optical properties (extinction, backscatter coefficient and depolarization ratio) and atmospheric structures like the planetary boundary layer (PBL), aerosol layers and clouds, with a line of sight resolution close to 15 m. With a 15 cm diameter telescope, the lidar is compact (~70 × 45 × 18 cm) and lightweight (<50 kg for both optics and electronics) and can thus be easily mounted aboard an aircraft. The wide field-of-view (FOV) ~2.3 mrad ensures a full-overlap of the transmit and receive paths beyond ~200 m.

2.2 The lidar signal

For a perfect separation of the 2 polarizations, the range corrected lidar signals $S^{1(2)}$ at the emitted wavelength λ for both the co-polarization ($//$, channel 1) and the cross-polarization (\perp , channel 2) channels is given at the distance r from the aircraft by (Measures, 1984)

$$S^{1(2)}(r) = C^{1(2)} \cdot (\beta_m^{1(2)}(r) + \beta_a^{1(2)}(r)) \cdot \exp\left(-2 \cdot \int_0^r (\alpha_m(r') + \alpha_a(r')) \cdot dr'\right). \quad (1)$$

The molecular (resp. aerosol) contribution is characterized by both the extinction α_m (resp. α_a) and the backscatter coefficients $\beta_m^{1(2)}$ (resp. $\beta_a^{1(2)}$). The molecular extinction and backscatter are known functions of the air density and can thus be predicted with a good accuracy from a climatological profile of air density, a weather analysis, a radiosounding, or a simple polynomial approximation as proposed by Nicolet (1984). $C^{1(2)}$ are the instrumental constants for each channel.

French airborne lidar measurements for Eyjafjallajökull ash plume survey

P. Chazette et al.

Title Page

Abstract

Introduction

Conclusions

References

Tables

Figures

⏪

⏩

◀

▶

Back

Close

Full Screen / Esc

Printer-friendly Version

Interactive Discussion



Taking into account that the two Brewster plates used for the separation of the two polarizations are not perfect (Fig. 1), the total elastic lidar signal must be computed from the two polarized signals by using the equation

$$S(r) = \frac{S^1(r) \cdot (1 + \text{VDR}(r))}{C^1 \cdot (T_1^{//} + T_1^\perp \cdot \text{VDR}(r))} \quad (2)$$

5 where VDR is the volume depolarization ratio

$$\text{VDR}(r) = \frac{R_c \cdot (1 - T_1^{//}) \cdot (1 - T_2^{//}) \cdot S^1(r) - T_1^{//} \cdot S^2(r)}{T_1^\perp \cdot S^2(r) - R_c \cdot (1 - T_1^\perp) \cdot (1 - T_2^\perp) \cdot S^1(r)} \quad (3)$$

$T_i^{//}$ and T_i^\perp are the transmissions of the co-polarization and cross-polarization contributions of the Brewster plate i , respectively. The cross-calibration coefficient $R_c = C^2 / C^1$ can be assessed by looking at the lidar signals obtained in a “clean” atmospheric volume with negligible aerosol content. There, the lidar signal is due solely to the known molecular backscatter between 6 and 7 km above the mean sea level (a.m.s.l.). The molecular volume depolarization ratio (VDR_m) was taken equal to 0.3945 % at 355 nm following Collis and Russel (1976). Because of the narrow width of the interferential filter (0.3 nm) of the receiver, only Cabannes scattering is observed by the lidar. The mean relative uncertainty on the cross-calibration coefficient was assessed before the flights over the Paris area and compared to the one of another ground-based lidar (GBL) used to follow the ash plume (Chazette et al., 2011). These measurements performed during the night of 19 April 2010 (23:00 LT) are shown in Fig. 2. The vertical profiles of apparent backscatter $\beta_{\text{app}}^{//(\perp)}$ ($S^{1(2)}$ corrected from the molecular transmission) derived from the two lidars are in very good agreement. After taking into account R_c for each lidar ($T_1^{//} = 0.77$ (0.90), $T_1^\perp = 0.0007$ (0.0012), $T_2^{//} = 0.77$ (0.90) and $T_2^\perp = 0.0009$ (0.0009) for the AL, GBL), the derived VDR are very similar. The mean relative uncertainty on R_c is $\sim 7\%$. The value of R_c may vary with the temperature and it is thus

French airborne lidar measurements for Eyjafjallajökull ash plume survey

P. Chazette et al.

Title Page

Abstract

Introduction

Conclusions

References

Tables

Figures



Back

Close

Full Screen / Esc

Printer-friendly Version

Interactive Discussion



necessary to assess R_c for each flight. At ground, we found $R_c = 16 \pm 0.49$ but this value evolved when the lidar was flying: 6.4 ± 0.07 on 21 April 2010 with a high temperature in the cockpit ($\sim 30^\circ\text{C}$), 10.4 ± 0.15 and 10.8 ± 0.10 on 12 and 16 May 2010, respectively, with cooler temperatures inside the cabin ($\sim 18^\circ\text{C}$). Between the last two flights R_c was very stable.

2.3 Retrieval of the ash plume optical properties

The retrieval of the ash optical properties from the AL is performed in two steps. In the first step, the aerosol optical thickness (AOT) of the ash layer plume is assessed (if possible). The second step consists of the inversion of a lidar equation. As it is well known, the inversion of lidar equation is an ill-posed problem as it contains two unknowns for a single equation. An additional constraint is thus needed. For an airborne lidar, such a constraint can be found when the aerosol plume is boarded by two atmospheric layers where only molecular scattering occurs. This specific situation has been encountered during our flights. Then the ash AOT can be easily written as

$$\begin{aligned} \text{AOT} &= \int_{z_b}^{z_a} \alpha_a(z) \cdot dz \\ \text{AOT} &= \frac{1}{2} \cdot \ln \left(\frac{\beta_m(z_a)}{\beta_m(z_b)} \cdot \frac{S(z_b)}{S(z_a)} \right) - \int_{z_b}^{z_a} \alpha_m(z) \cdot dz \end{aligned} \quad (4)$$

where z is the altitude a.m.s.l. ($z = z_f - r \cos(\theta)$ with z_f the aircraft altitude and θ the pointing angle relative to nadir); z_b and z_a are the altitudes within the molecular layers beneath and above the ash plume, respectively. Using the backscatter to extinction ratio (BER, inverse of the lidar ratio LR), the elastic Eq. (1) becomes a differential equation of type Bernoulli first order and can be mathematically inverted (Klett, 1985)

$$\alpha_a(z) = \text{BER}^{-1} \left(\frac{S(z)Q(z)}{\frac{S(z_b)}{(\beta_m(z_b) + \beta_a(z_b))} + 2 \cdot \text{BER}^{-1} \int_{z_b}^z S(z')Q(z')dz'} - \beta_m(z) \right). \quad (5)$$

French airborne lidar measurements for Eyjafjallajökull ash plume survey

P. Chazette et al.

Title Page

Abstract

Introduction

Conclusions

References

Tables

Figures

⏪

⏩

◀

▶

Back

Close

Full Screen / Esc

Printer-friendly Version

Interactive Discussion



Here, Q is the correction factor related to the differential molecular optical thickness calculated from the vertical profile of the molecular scattering coefficient as

$$Q(z) = \exp\left(2 \left[k_f \frac{3}{8\pi \cdot \text{BER}} - 1 \right] \int_{z_b}^z \alpha_m(z') dz' \right) \quad (6)$$

where k_f is the King factor of air (King, 1923). Considering $k_f = 1$ leads to an overestimation on the molecular volume backscatter coefficient of only 1.5 % at 355 nm (Collis and Russel, 1976). BER is assessed using the AOT as a constraint in Eq. (5) via a dichotomy approach as described by Chazette (2003) or Royer et al. (2010). The value hence retrieved is constant for the entire ash layer. This assumes that the ashes are distributed homogeneously across the plume.

The uncertainties in the determination of AOT, α_a and BER can be related to three main sources: (i) the detection noise (shot noise, electronic noise...), (ii) the presence of residual aerosols in the altitude ranges used for lidar calibration, (iii) the uncertainty on the a priori knowledge of the vertical profile of the Rayleigh backscatter coefficient as determined from ancillary measurements. This last uncertainty is negligible (<2 % on α_a or BER) compared to the others. The statistical uncertainties on the ash optical parameters have been calculated (see Sect. 4.1) using a Monte Carlo approach as in Chazette (2003). Due to the distance between the emitter and the scattering layer, the field of view, and the AOT value (see below), the multiple scattering effects can be neglected in comparison to the other sources of uncertainty.

The higher contribution of the molecular scattering at 355 nm leads to prefer the particulate depolarization ratio (PDR) to characterize the ash depolarization properties linked to their non-sphericity. The PDR is given by (Chazette et al., 2011)

$$\text{PDR}(z) = \frac{\beta_m(z) \cdot (\text{VDR}_m - \text{VDR}(z)) - \beta_a(z) \cdot \text{VDR}(z) \cdot (1 + \text{VDR}_m)}{\beta_m(z) \cdot (\text{VDR}(z) - \text{VDR}_m) - \beta_a(z) \cdot (1 + \text{VDR}_m)} \quad (7)$$

French airborne lidar measurements for Eyjafjallajökull ash plume survey

P. Chazette et al.

Title Page

Abstract

Introduction

Conclusions

References

Tables

Figures

⏪

⏩

◀

▶

Back

Close

Full Screen / Esc

Printer-friendly Version

Interactive Discussion



The PDR is generally very noisy because it is the ratio of two noisy functions of β_a . Hence, its assessment is restricted to high values of aerosol extinction coefficient ($>0.1 \text{ km}^{-1}$ for our AL).

3 Flights plans and ash plume identification

5 Probable presence of volcanic ash was detected during three flights of the F-20. These flights were carried out on 21 April, 12 and 16 May 2010, inside the French, Spanish and British air spaces, respectively. The aircraft took off from the military airport of Toulouse-Francazal for each of them, and landed on the same airport. The volcanic ash plume has been mainly identified using the perpendicular channel of the airborne
10 lidar, in terms of β_{app}^\perp .

On 21 April 2010, while air traffic was resuming over France, a thin volcanic aerosol layer was measured in the Northern part of France above a cloud layer between Strasbourg and Dieppe (Fig. 3). The AOT of the ash plume was lower than 0.03 at 355 nm. It is thus very difficult to retrieve the ash optical properties. The VDR is $\sim 5\%$ showing the
15 presence of ash in agreement with the previous measurements performed by Chazette et al. (2011). Moreover, there is no molecular layer beneath the ash plume. Hereafter, we do not consider these lidar measurements for a quantitative study.

The second flight was over the Atlantic Ocean, off the Spanish coast (La Coruna), towards the West as shown Fig. 4. A filament ($\sim 500 \text{ m}$ thick) with a high density
20 was first observed by the AL (located between -9.82 and -12.06° in longitude and at $\sim 5 \text{ km a.m.s.l.}$ in Fig. 4). But the main body of the volcanic plume was found further west at about the limit of range of the aircraft ($\sim 1200 \text{ km}$ off La Coruna). Therefore only the edge of the plume could be observed by the AL. It extends vertically from 2 to $\sim 7 \text{ km a.m.s.l.}$ Lidar signals are reported in Fig. 4. The figure is nearly symmetrical
25 as the aircraft flew a return flight along almost the same route. The backtrajectories computed with the HYSPLIT (Hybrid Single Particle Lagrangian Integrated Trajectory Model) model (courtesy of NOAA Air Resources Laboratory; <http://www.arl.noaa.gov>)

French airborne lidar measurements for Eyjafjallajökull ash plume survey

P. Chazette et al.

Title Page

Abstract

Introduction

Conclusions

References

Tables

Figures

⏪

⏩

◀

▶

Back

Close

Full Screen / Esc

Printer-friendly Version

Interactive Discussion



are shown in Fig. 5. The ashes that were present within the filament and the plume were not emitted on the same day (10 May for the filament and 11 May for the plume) neither advected with the same efficiency. For the filament, the main contribution to the lidar signal came from an altitude of ~ 2 km a.m.s.l., whereas it came between 4 and 5 km a.m.s.l. for the main plume.

On 16 May, the British air space was closed. Volcanic ashes were expected and encountered in the North of England. The ash plume is well located by the AL measurements as shown Fig. 6. It lies between ~ 3 and 6 km a.m.s.l. Backtrajectories, from different end-points, within the ash plume are displayed in Fig. 7. They confirm the source of the ash plume as being the Eyjafjallajökull volcano.

Note that the ubiquitous cloud cover during the flights makes it difficult to identify ash plumes from space. Few cloud-free pixels are available on SEVERI or MODIS (not shown) and backtrajectories appear as the most relevant means to identify the origin of the ash layers detected from the AL.

4 Optical properties and mean ash mass concentration

The calculations have been performed on mean profiles measured in the ash plumes for which we have two molecular normalization points, above and beneath the plume (z_a and z_b , respectively). Such an averaging can significantly improve the signal to noise ratio (SNR) in the molecular zones to reach values larger than 10 needed for an accurate inversion (Table 2). The assessment of the ash optical properties does not require assumptions about the chemical nature and morphological properties of the ash. This is not the case for the assessment of the ash mass concentrations (e.g. Gasteiger et al., 2011; Chazette et al., 2011).

French airborne lidar measurements for Eyjafjallajökull ash plume survey

P. Chazette et al.

Title Page

Abstract

Introduction

Conclusions

References

Tables

Figures

⏪

⏩

◀

▶

Back

Close

Full Screen / Esc

Printer-friendly Version

Interactive Discussion



4.1 Optical parameters

The range-corrected mean lidar signal is given in Fig. 8 for 12 and 16 May 2010. For 12 May, we have firstly distinguished the plume from the filament, and secondly we have considered separately the plume-crown, located between ~ 5 and 7 km a.m.s.l., from the plume itself, which is located below, between ~ 2 and 5 km a.m.s.l. (Fig. 5). Note that the lower molecular reference altitude is lower boarded by cloud signatures.

4.1.1 Aerosol Optical Thickness in the plume

The AOTs at 355 nm retrieved from Eq. (4) for each case are given in Table 2. The event on 16 May is the most intense with AOT = 0.34 compared with the ash plumes observed on 12 May with AOT of 0.19, 0.08 and 0.16 for the plume, plume-crown and filament, respectively. The lower molecular reference z_b is very likely to be contaminated by residual aerosol contribution and the AOTs are likely biased. It is unclear whether aerosols are a priori present at the molecular reference level. Hence, the potential bias on the AOT (δ_{AOT}) was assessed using two scattering coefficients ($R = 1 + \beta_a / \beta_m$) at the lower molecular reference altitude. The results are presented in Table 2 for $R = 1.05$ and $R = 1.09$. At the molecular reference z_b , $R = 1.05$ (1.09) leads to a bias on the lidar signal at least equal to the (twice) signal noise level. Such a deviation is assumed to be observable on the profiles of Fig. 8. For $R = 1.05$, the bias ($\delta_{\text{AOT}} \sim -0.02$) on the AOT is the same whatever the AOT values. The bias is more than twice as important as for $R = 1.09$ (between 0.04 and 0.05). The statistical uncertainty (ε_{AOT}) linked to the signal noise is low (less than 3 %, Table 2).

4.1.2 Aerosol extinction coefficient profiles

Given the AOT of the ash plumes, the AL measurements on 12 and 16 May were converted into extinction coefficients using both the Klett (1985) backward algorithm and the dichotomy approach. The mean vertical profiles of aerosol extinction coefficient

Title Page

Abstract

Introduction

Conclusions

References

Tables

Figures

⏪

⏩

◀

▶

Back

Close

Full Screen / Esc

Printer-friendly Version

Interactive Discussion



are given in Fig. 9. The vertical structure can be complex as on 12 May with several maxima above 0.1 km^{-1} . The maximum extinction coefficient is given in Table 2 for each mean profile. The values are between 0.21 and 0.44 km^{-1} for the plume-crown and the filament of 12 May, respectively. The ash plume of 16 May has a maximum α_a of 0.30 km^{-1} . The statistic uncertainty ε_α and the absolute value of the bias δ_α ($R = 1.05$) are lower than 2 and 6 %, respectively (Table 2).

4.1.3 Backscatter-to-Extinction Ratio in the plume

The BER retrieved from AL measurements are also given in Table 2. The values between 0.021 and 0.025 sr^{-1} (LR between 40 and 47.6 sr) are very close to those measured with ground-based Raman lidar near Paris (0.021 sr^{-1} , Royer et al., 2010) except for the filament (BER = 0.030 sr^{-1} or LR = 33.3 sr). This may be due to the presence of ice-nuclei within the ash filament as observed from airborne in situ measurements over UK by Schumann et al. (2011).

The LR in the ash plume retrieved in this study is close to the LR values of 50 ± 5 assessed by Ansmann et al. (2010) for Munich. The same authors measured LR = 60 ± 5 sr at Leipzig, which is larger than our values. The statistic error (ε_{BER}) on the BER is low ($<3\%$) but the bias (δ_{BER}) linked to $R = 1.05$ may significantly overestimate the BER by 26 % for the lower AOT of 0.08 (Table 2). Note that a value of $R = 1.09$ doubles the bias on each parameters as shown Table 2.

4.1.4 Depolarization measurements

The last optical parameter that we have assessed is the PDR (Eq. 7) derived from the VDR (Eq. 3). Figure 10 gives the mean vertical profiles of both the VDR and the PDR when the SNR is large enough. Marengo and Hogan (2011) performed ground-based elastic-backscattering lidar measurements at Exeter, United Kingdom, on 16 and 18 April 2010. They found VDR between 10 and 20 % in agreement with the value shown Fig. 10. When working at the wavelength of 355 nm where molecular scattering

French airborne lidar measurements for Eyjafjallajökull ash plume survey

P. Chazette et al.

Title Page

Abstract

Introduction

Conclusions

References

Tables

Figures

⏪

⏩

◀

▶

Back

Close

Full Screen / Esc

Printer-friendly Version

Interactive Discussion

French airborne lidar measurements for Eyjafjallajökull ash plume survey

P. Chazette et al.

Title Page

Abstract

Introduction

Conclusions

References

Tables

Figures

⏪

⏩

◀

▶

Back

Close

Full Screen / Esc

Printer-friendly Version

Interactive Discussion



is high, the best representative depolarization ratio is the PDR. When encompassing all the PDR profiles, the mean value is very stable, between 42 ± 5 and 47 ± 7 % (Table 2). These values are inside the range derived by Chazette et al. (2011) from GBL measurements. They are higher than the results of Ansmann et al. (2011) or Gasteiger et al. (2011) that retrieved mean PDR at the same wavelength of 35–40 % and 35.5 ± 4.4 %, respectively. The ash plumes may evolve during transport by particle settling and their optical properties may be affected. Note that for the ash plume observed during the flights in May, the residence time in the atmosphere was less than 3 days (Figs. 5 and 7). Moreover, the ash plume is very heterogeneous and the ash properties could be different from an eruption to another. This may explain that the ash optical properties are not necessary the same from a location to another, and from a time to another.

4.2 Ash mass concentration

A mass concentration estimate is a major requirement for aviation and for modeling purposes (e.g. Stohl et al., 2011). Nevertheless, no measurement of the ash microphysical properties has been performed from the F-20 because the flights were dedicated to the ash plume tracking by the AL. Therefore we use the specific cross section (σ_s) of ash assessed from the previous literature on the Eyjafjallajökull volcano. The Table 3 summarizes these values, which are widely dispersed, between 0.19 and $1.5 \text{ m}^2 \text{ g}^{-1}$. The higher values are retrieved by Hogan et al. (2012), Gasteiger et al. (2011) and Johnson et al. (2012) and belong to the intervals from 1 to $1.5 \text{ m}^2 \text{ g}^{-1}$, 0.43 to $1.15 \text{ m}^2 \text{ g}^{-1}$ and 0.45 to $1.06 \text{ m}^2 \text{ g}^{-1}$, respectively. Note that σ_s is close to $1.1 \text{ m}^2 \text{ g}^{-1}$ for dust particles originating from Sahara (e.g. Raut and Chazette, 2009), hence σ_s for dust aerosol can be considered as the upper boundary for ash. The lower value is given by Chazette et al. (2011) for ash plume over the Paris area with $\sigma_s = 0.19\text{--}0.29 \text{ m}^2 \text{ g}^{-1}$. As shown by the previous authors, these values leads to coherent comparison with the Eulerian model Polair3D transport model. Intermediate values are given by Ansmann et

al. (2010) with $\sigma_s \sim 0.43 \text{ m}^2 \text{ g}^{-1}$, and Ansmann et al. (2011) with $\sigma_s \sim 0.66 \text{ m}^2 \text{ g}^{-1}$ from the coupling between sunphotometer and a GBL.

Using the specific cross-sections between 0.19 and $1.1 \text{ m}^2 \text{ g}^{-1}$ in the equation

$$\text{AMC} = \frac{\max(\alpha_a)}{\sigma_s} \text{ and } \text{AMIC} = \frac{\text{AOT}}{\sigma_s}, \quad (8)$$

we have assessed both the ash mass concentrations (AMC) and the ash mass integrated concentration (AMIC) over the plumes. The values are reported in Table 2 (corresponding to the maximum of α_a for AMC). For 12 May, the AMC (AMIC) varies from 190 to $2160 \mu\text{g m}^{-3}$ (70 to 1000 mg m^{-2}) in the plume, and from 400 to $2300 \mu\text{g m}^{-3}$ (145 to 840 mg m^{-2}) in the filament. Similar values are retrieved for 16 May with an AMC between 270 and $1600 \mu\text{g m}^{-3}$, and an AMIC between 310 and 1800 mg m^{-2} .

5 Conclusions

Three operational flights were carried out with a Rayleigh-Mie lidar aboard the F-20 French research aircraft. The original purpose of these flights was to provide the French civil aviation authorities with objective information on the presence and location of ash plumes. The volcanic aerosol layers were identified mainly by using the perpendicular channel of the AL.

Ash plumes have been characterized by their PDR, which is very constant from a flight to another with value between 42 and 47% . The detected ash plumes are very similar in term of optical properties except the ash filament observed on 12 May, which stayed longer in the atmosphere than the main plume. For the ash plumes, the backscatter ratio (lidar ratio) appears to be coherent with the previous finding with values between 0.021 to 0.025 sr^{-1} (40 and 47.6 sr). The maximum AMC (between 190 and $2300 \mu\text{g m}^{-3}$ based on the likely range of the specific cross-section) may be rather less than or of the order of the critical level of damage given by the aircraft

French airborne lidar measurements for Eyjafjallajökull ash plume survey

P. Chazette et al.

Title Page

Abstract

Introduction

Conclusions

References

Tables

Figures

⏪

⏩

◀

▶

Back

Close

Full Screen / Esc

Printer-friendly Version

Interactive Discussion



engine manufacturers (2 mg m^{-3}) for the aircraft engines. Nevertheless, the $200 \mu\text{g m}^{-3}$ warning level was significantly reached.

The AL is thus utterly suitable for ash identification. Its measurements encompassed all the aerosol layers of the troposphere and are a powerful asset in the frame of a decision making tool. It supplied vertical profiles essential for the localization, the identification and the assessment of the ash content. In both April and May 2010, it enabled to confirm air traffic reopening over the French airspace.

Acknowledgements. The SAFIRE team is greatly acknowledged for its effectiveness in the implementation of research aircraft and its support for the integration of lidar and its participation in the different flights. This work was supported by the Commissariat à l'Energie Atomique (CEA). The "Centre National d'Etudes Spatiales" (CNES), Météo-France and the "Institut des Sciences de l'Univers" (INSU) supported the achievement of the airborne experience.



The publication of this article is financed by CNRS-INSU.

References

Ansmann, A., Tesche, M., Gross, S., Freudenthaler, V., Seifert, P., Hiebsch, A., Schmidt, J., Wandinger, U., Mattis, I., Müller, D., and Wiegner, M.: The 16 April 2010 major volcanic ash plume over central Europe: EARLINET lidar and AERONET photometer observations at Leipzig and Munich, Germany, *Geophys. Res. Lett.*, 37, L13810, doi:10.1029/2010GL043809, 2010.

Ansmann, A., Tesche, M., Seifert, P., Groß, S., Freudenthaler, V., Apituley, A., Wilson, K. M., Serikov, I., Linné, H., Heinold, B., Hiebsch, A., Schnell, F., Schmidt, J., Mattis, I., Wandinger,

French airborne lidar measurements for Eyjafjallajökull ash plume survey

P. Chazette et al.

Title Page

Abstract

Introduction

Conclusions

References

Tables

Figures

⏪

⏩

◀

▶

Back

Close

Full Screen / Esc

Printer-friendly Version

Interactive Discussion



French airborne lidar measurements for Eyjafjallajökull ash plume survey

P. Chazette et al.

Title Page

Abstract

Introduction

Conclusions

References

Tables

Figures

⏪

⏩

◀

▶

Back

Close

Full Screen / Esc

Printer-friendly Version

Interactive Discussion

- U., and Wiegner, M.: Ash and fine-mode particle mass profiles from EARLINET- AERONET observations over central Europe after the eruptions of the Eyjafjallajökull volcano in 2010, *J. Geophys. Res.*, 116, D00U02, doi:10.1029/2010JD015567, 2011.
- 5 Bukowiecki, N., Zieger, P., Weingartner, E., Jurányi, Z., Gysel, M., Neininger, B., Schneider, B., Hueglin, C., Ulrich, A., Wichser, A., Henne, S., Brunner, D., Kaegi, R., Schwikowski, M., Tobler, L., Wienhold, F. G., Engel, I., Buchmann, B., Peter, T., and Baltensperger, U.: Ground-based and airborne in-situ measurements of the Eyjafjallajökull volcanic aerosol plume in Switzerland in spring 2010, *Atmos. Chem. Phys.*, 11, 10011–10030, doi:10.5194/acp-11-10011-2011, 2011.
- 10 Chazette, P.: The monsoon aerosol extinction properties at Goa during INDOEX as measure with lidar, *J. Geophys. Res.*, 108, 4167, doi:10.1029/2002JD002074, 2003.
- Chazette, P., David, C., Lefrère, J., Godin, S., Pelon, J., and Mégie, G.: Comparative lidar study of the optical, geometrical, and dynamical properties of stratospheric post-volcanic aerosols, following the eruption of El Chichon and Mount Pinatubo, *J. Geophys. Res.*, 100, 23195–23207, 1995.
- 15 Chazette, P., Sanak, J., and Dulac, F.: New Approach for Aerosol Profiling with a Lidar Onboard an Ultralight Aircraft: Application to the African Monsoon Multidisciplinary Analysis, *Environ. Sci. Technol.*, 41, 8335–8341, 2007.
- Chazette, P., Bocquet, M., Royer, P., Winiarek, V., Raut, J.-C., Labazuy, P., Gouhier, M., Lardier, M., and Cariou, J.-P.: Eyjafjallajökull ash concentrations derived from both lidar and modeling, *J. Geophys. Res.*, online first: doi:10.1029/2011JD015755, 2011.
- 20 Collis, R. T. H. and Russell, P. B.: Lidar measurement of particles and gases by elastic backscattering and differential absorption in *Laser Monitoring of the Atmosphere*, edited by: Hinkley, E. D., 71–152, Springer-Verlag, New York, 1976.
- 25 Gasteiger, J., Gro, S., Freudenthaler, V., and Wiegner, M.: Volcanic ash from Iceland over Munich: mass concentration retrieved from ground-based remote sensing measurements, *Atmos. Chem. Phys.*, 11, 2209–2223, doi:10.5194/acp-11-2209-2011, 2011.
- Gertisser, R.: Eyjafjallajökull volcano causes widespread disruption to European air traffic, *Geol. Today*, 26, 94–95, 2010.
- 30 Hogan, R. J., Haywood, J. M., Westbrook, C. D., Dacre, H. F., Marengo, F., O'Connor, E. J., Johnson, B. T., Wrench, C. L., and Belcher, S. E.: Combined lidar and sunphotometer retrievals of ash particle size and mass concentration from the Eyjafjallajökull volcano, *J. Geophys. Res.*, in press, 2012.

French airborne lidar measurements for Eyjafjallajökull ash plume survey

P. Chazette et al.

[Title Page](#)[Abstract](#)[Introduction](#)[Conclusions](#)[References](#)[Tables](#)[Figures](#)[⏪](#)[⏩](#)[◀](#)[▶](#)[Back](#)[Close](#)[Full Screen / Esc](#)[Printer-friendly Version](#)[Interactive Discussion](#)

- Jäger, H.: The Pinatubo eruption cloud observed by lidar at Garmisch-Partenkirchen, *Geophys. Res. Lett.*, 19, 191–194, 1992.
- Johnson, B., Turnbull, K., Dorsey, J., Baran, A. J., Ulanowski, Z., Hesse, E., Cotton, R., Brown, P. R. A., Burgess, R., Capes, G., Webster, H., Woolley, A., Rosenberg, P., and Haywood, J. M.: In situ observations of volcanic ash clouds from the FAAM aircraft during the eruption of Eyjafjallajökull in 2010, *J. Geophys. Res.*, in press, 2012.
- King, L. V.: On the complex anisotropic molecule in relation to the dispersion and scattering of light, *P. R. Soc. London, Series 1*, 104, 333–357, 1923.
- Klett, J. D.: Lidar inversion with variable backscatter/extinction ratios, *Appl. Optics*, 24, 1638–1643, 1985.
- Marenco, F. and Hogan, R.: Determining the contribution of volcanic ash and boundary-layer aerosol in backscatter lidar returns: A three-component atmosphere approach, *J. Geophys. Res.*, 116, D00U06, doi:10.1029/2010JD015415, 2011.
- Marenco, F., Johnson, B., Turnbull, K., Newman, S., Haywood, J., Webster, H., and Ricketts, H.: Airborne lidar observations of the 2010 Eyjafjallajökull volcanic ash plume, *J. Geophys. Res.*, 116, D00U05, doi:10.1029/2011JD016396, 2011.
- Measures, R. M.: *Laser remote sensing: Fundamentals and Applications*, Wiley & Sons, NewYork, 1984.
- Millington, S. C., Saunders, R. W., and Francis, P. N.: Simulated SEVIRI volcanic ash imagery, *J. Geophys. Res.*, online first: doi:10.1029/2011JD016770, 2011.
- Nicolet, M.: On the molecular scattering in the terrestrial atmosphere, *Planet. Space Sci.*, 32, 1467–1468, doi:10.1016/0032-0633(84)90089-8, 1984.
- Osborn, M. T., Winker, D. M., Woods, D. C., DeCoursey, R. J., and Trepte, C. R.: Evolution of the Pinatubo volcanic cloud over Hampton, Virginia, *Geophys. Res. Lett.*, 22, 1101–1104, 1995.
- Prata, A. J., Gangale, G., Clarisse, L., and Karagulian, F.: Ash and sulfur dioxide in the 2008 eruptions of Okmok and Kasatochi: Insights from high spectral resolution satellite measurements, *J. Geophys. Res.*, 115, D00L18, doi:10.1029/2009JD013556, 2010.
- Raut, J.-C. and Chazette, P.: Assessment of vertically-resolved PM₁₀ from mobile lidar observations, *Atmos. Chem. Phys.*, 9, 8617–8638, doi:10.5194/acp-9-8617-2009, 2009.
- Royer, P., Chazette, P., Lardier, M., and Sauvage, L.: Aerosol content survey by mini-N2-Raman lidar: Application to local and long-range transport aerosols, *Atmos. Environ.*, doi:10.1016/j.atmosenv.2010.11.001, 2011.

French airborne lidar measurements for Eyjafjallajökull ash plume survey

P. Chazette et al.

Title Page

Abstract

Introduction

Conclusions

References

Tables

Figures

⏪

⏩

◀

▶

Back

Close

Full Screen / Esc

Printer-friendly Version

Interactive Discussion



- Schumann, U., Weinzierl, B., Reitebuch, O., Schlager, H., Minikin, A., Forster, C., Baumann, R., Sailer, T., Graf, K., Mannstein, H., Voigt, C., Rahm, S., Simmet, R., Scheibe, M., Lichtenstern, M., Stock, P., Rüba, H., Schäuble, D., Tafferner, A., Rautenhaus, M., Gerz, T., Ziereis, H., Krautstrunk, M., Mallaun, C., Gayet, J.-F., Lieke, K., Kandler, K., Ebert, M., Weinbruch, S., Stohl, A., Gasteiger, J., Gro, S., Freudenthaler, V., Wiegner, M., Ansmann, A., Tesche, M., Olafsson, H., and Sturm, K.: Airborne observations of the Eyjafjalla volcano ash cloud over Europe during air space closure in April and May 2010, *Atmos. Chem. Phys.*, 11, 2245–2279, doi:10.5194/acp-11-2245-2011, 2011.
- Sigmundsson, F., Hreinsdottir, S., Hooper, A., Arnadottir, T., Pedersen, R., Roberts, M. J., Oskarsson, N., Auriac, A., Deciem, J., Einarsson, P., Geirsson, H., Hensch, M., Ofeigsson, B. G., Sturkell, E., Sveinbjornsson, H., and Feigl, K. L.: Intrusion triggering of the 2010 Eyjafjallajökull explosive eruption, *Nature*, 468, 426–430, 2010.
- Stohl, A., Prata, A. J., Eckhardt, S., Clarisse, L., Durant, A., Henne, S., Kristiansen, N. I., Minikin, A., Schumann, U., Seibert, P., Stebel, K., Thomas, H. E., Thorsteinsson, T., Tørseth, K., and Weinzierl, B.: Determination of time- and height-resolved volcanic ash emissions and their use for quantitative ash dispersion modeling: the 2010 Eyjafjallajökull eruption, *Atmos. Chem. Phys.*, 11, 4333–4351, doi:10.5194/acp-11-4333-2011, 2011.
- Thomas, H. E. and Watson, I. M.: Observations of volcanic emissions from space: Current and future perspectives, *Nat. Hazards*, 54, 323–354, 2010.
- Winker, D. M. and Osborn, M. T.: Airborne Lidar Observations of the Pinatubo Volcanic Plume, *Geophys. Res. Lett.*, 19, 167–170, 1992.

French airborne lidar measurements for Eyjafjallajökull ash plume survey

P. Chazette et al.

Table 1. Main characteristic of the airborne lidar system.

Characteristics	Details
Lidar head size	~65 × 35 × 18 cm
Lidar head and electronic weight	~40 kg
Laser type	Nd:YAG 20 Hz 16 mJ @ 355 nm
Laser pulse length	~5–7 ns
Laser divergence	0.1 mrad
Reception channels	Elastic 355 nm // et ⊥
Reception diameter	150 mm
Field of view	~2.3 mrad
Full-overlap	200 m
Detector	Photomultiplier (analog mode)
Filter bandwidth	0.3 nm
Electronic system	PXI 200 MHz
Vertical sampling (resolution)	1.5 m (15 m)

[Title Page](#)
[Abstract](#)
[Introduction](#)
[Conclusions](#)
[References](#)
[Tables](#)
[Figures](#)
[⏪](#)
[⏩](#)
[◀](#)
[▶](#)
[Back](#)
[Close](#)
[Full Screen / Esc](#)
[Printer-friendly Version](#)
[Interactive Discussion](#)

French airborne lidar measurements for Eyjafjallajökull ash plume survey

P. Chazette et al.

Title Page

Abstract

Introduction

Conclusions

References

Tables

Figures

⏪

⏩

◀

▶

Back

Close

Full Screen / Esc

Printer-friendly Version

Interactive Discussion

Table 2. Optical properties of the ash plumes. The relative statistic uncertainties (ε_x) are given for each property x and plume type. The relative bias (δ_x) linked to the presence of aerosol at the altitude of normalization is also given.

Scattering coefficient		16 May	12 May Plume	12 May Plume-crown	12 May Filament
$R = 1$	SNR _b	12	12	19	14
	SNR _a	35	28	56	27
	BER	0.023 sr ⁻¹	0.025 sr ⁻¹	0.021 sr ⁻¹	0.030 sr ⁻¹
	max(α_a)	0.30 km ⁻¹	0.41 km ⁻¹	0.21 km ⁻¹	0.44 km ⁻¹
	PDR	44 ± 6	47 ± 7	42 ± 5	46 ± 7
	AOT	0.34	0.19	0.08	0.16
	ε_{AOT}	1.2 %	1.9 %	3.2 %	3 %
	ε_{BER}	1 %	1.7 %	2.8 %	2.7 %
	ε_α	2 %	2.8 %	12 %	3.2 %
$R = 1.05$	δ_{AOT}	-7 %	-12 %	-30 %	-14 %
	δ_{BER}	3 %	6 %	26 %	10 %
	δ_α	-6 %	-10 %	-24 %	-11 %
$R = 1.09$	δ_{AOT}	-12 %	-21 %	-58 %	-28 %
	δ_{BER}	5 %	11 %	87 %	24 %
	δ_α	-11 %	-17 %	-52 %	-22 %
Range of ash mass concentration ($\mu\text{g m}^{-3}$)	From	270	370	190	400
	to max(α_a)	1600	2160	1100	2300
Range of integrated mass concentration (mg m^{-2})	From	310	170	70	145
	to AOT	1800	1000	420	840

French airborne lidar measurements for Eyjafjallajökull ash plume survey

P. Chazette et al.

Table 3. Specific cross-section (σ_s) given in the literature.

Reference	σ_s ($\text{m}^2 \text{g}^{-1}$)	Wavelength (nm)	Location and period of measurements
Ansmann et al. (2010)	0.43	355 and 532	Leipzig and Munich, Germany April 2010
Gasteiger et al. (2011)	0.43–1.15	532	Munich, Germany April 2010
Ansmann et al. (2011)	0.66	532	Central Europe April and May 2010
Hogan et al. (2012)	1.25 ± 0.25	340, 355, 1020 and 1500	UK April 2010
Johnson et al. (2011)	0.45–1.06	355–680	UK April and May 2010
Chazette et al. (2011)	$0.19 \pm 0.03 - 0.29 \pm 0.04$	355	Paris, France April 2010

[Title Page](#)
[Abstract](#)
[Introduction](#)
[Conclusions](#)
[References](#)
[Tables](#)
[Figures](#)
[Back](#)
[Close](#)
[Full Screen / Esc](#)
[Printer-friendly Version](#)
[Interactive Discussion](#)

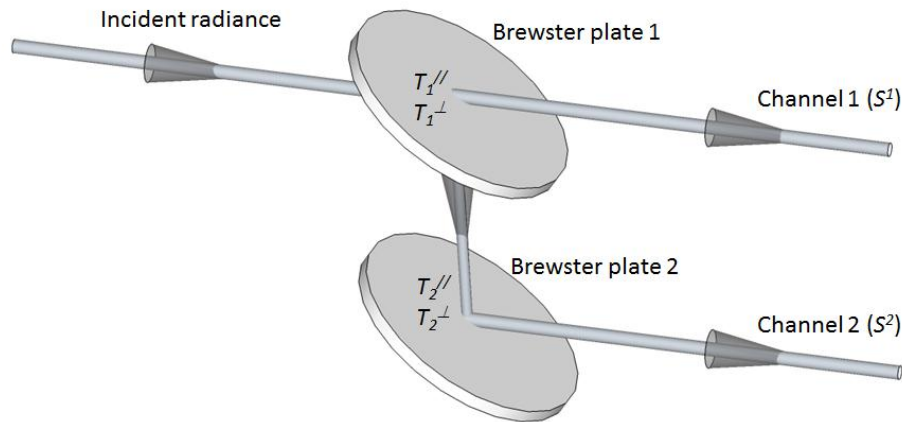


Fig. 1. Schematic representation of the co-polar and cross-polar channels.

French airborne lidar measurements for Eyjafjallajökull ash plume survey

P. Chazette et al.

Title Page

Abstract Introduction

Conclusions References

Tables Figures

◀ ▶

◀ ▶

Back Close

Full Screen / Esc

Printer-friendly Version

Interactive Discussion

French airborne lidar measurements for Eyjafjallajökull ash plume survey

P. Chazette et al.

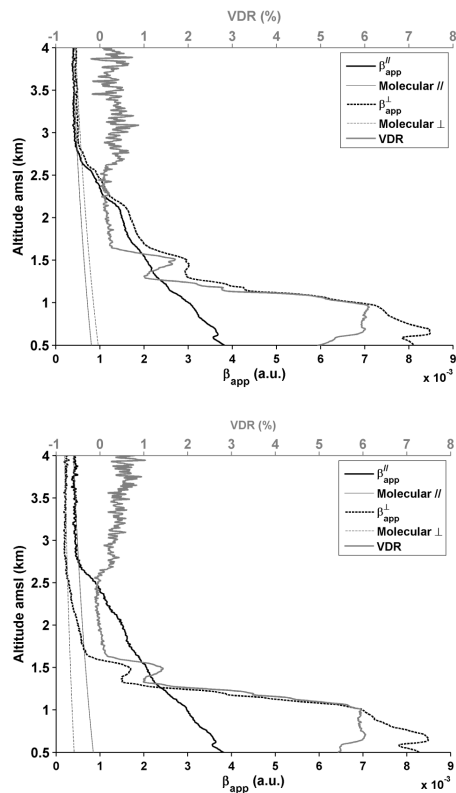


Fig. 2. Vertical profiles of the apparent backscatter coefficient $\beta_{app}^{\parallel/\perp}$ and VDR for the AL (top) and GBL (bottom). The molecular contribution is also indicated for the co-polar and cross-polar channels.

Title Page

Abstract

Introduction

Conclusions

References

Tables

Figures

◀

▶

◀

▶

Back

Close

Full Screen / Esc

Printer-friendly Version

Interactive Discussion

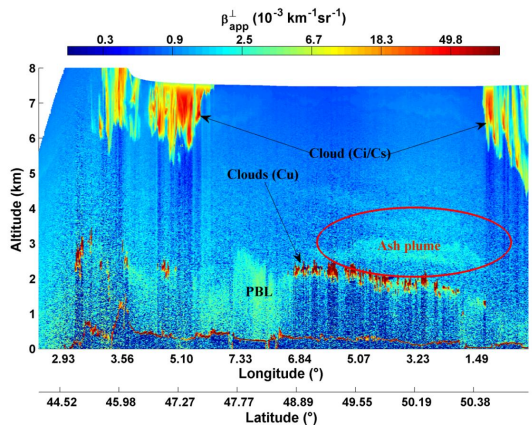
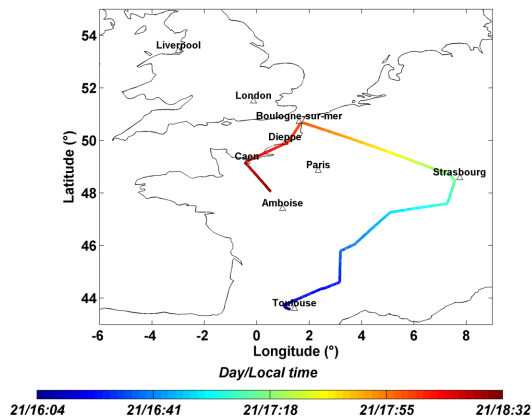


Fig. 3. Flight for 21 April 2010. Top panel shows the flight plane above France where the main crossed cities are given. Bottom panel shows the temporal evolution of β_{app}^{\pm} . The shallow ash plume is circled in red.

French airborne lidar measurements for Eyjafjallajökull ash plume survey

P. Chazette et al.

Title Page

Abstract Introduction

Conclusions References

Tables Figures

◀ ▶

◀ ▶

Back Close

Full Screen / Esc

Printer-friendly Version

Interactive Discussion

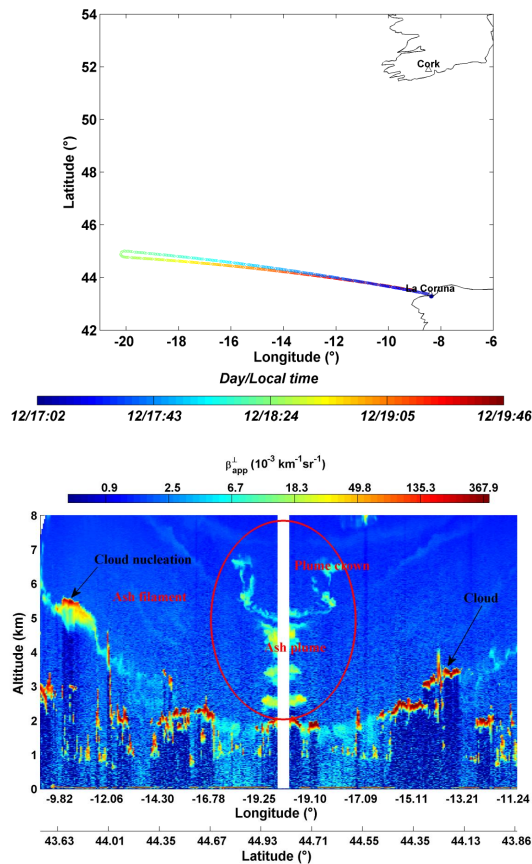


Fig. 4. The same as Fig. 3 for 12 May 2010, off La Coruna.

French airborne lidar measurements for Eyjafjallajökull ash plume survey

P. Chazette et al.

Title Page

Abstract Introduction

Conclusions References

Tables Figures

◀ ▶

◀ ▶

Back Close

Full Screen / Esc

Printer-friendly Version

Interactive Discussion



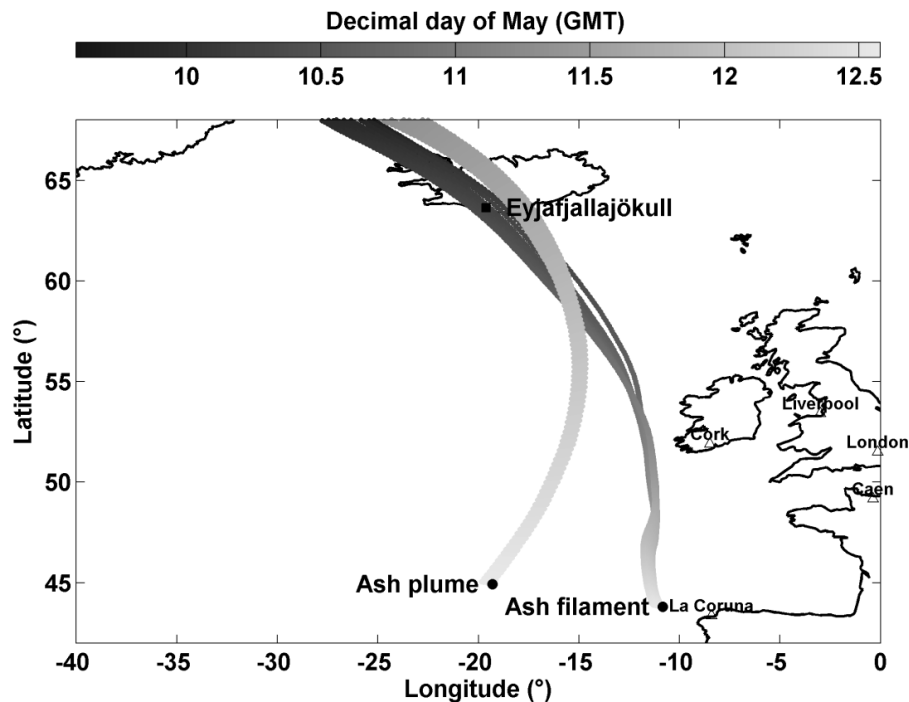


Fig. 5. Backtrajectories on 12 May 2010 computed using the Hysplit model (courtesy of NOAA Air Resources Laboratory; <http://www.arl.noaa.gov>). The wind fields are from GDAS (Global Data Assimilation System, <http://www.ncep.noaa.gov/>) at the horizontal resolution of 1°. Two terminal locations of the air masses are considered: one in the ash plume and the other one in the filament. All the lidar observations in the ash structures are considered as the individual final location of the air masses.

French airborne lidar measurements for Eyjafjallajökull ash plume survey

P. Chazette et al.

Discussion Paper | Discussion Paper | Discussion Paper | Discussion Paper | Discussion Paper

Title Page	
Abstract	Introduction
Conclusions	References
Tables	Figures
◀	▶
◀	▶
Back	Close
Full Screen / Esc	
Printer-friendly Version	
Interactive Discussion	



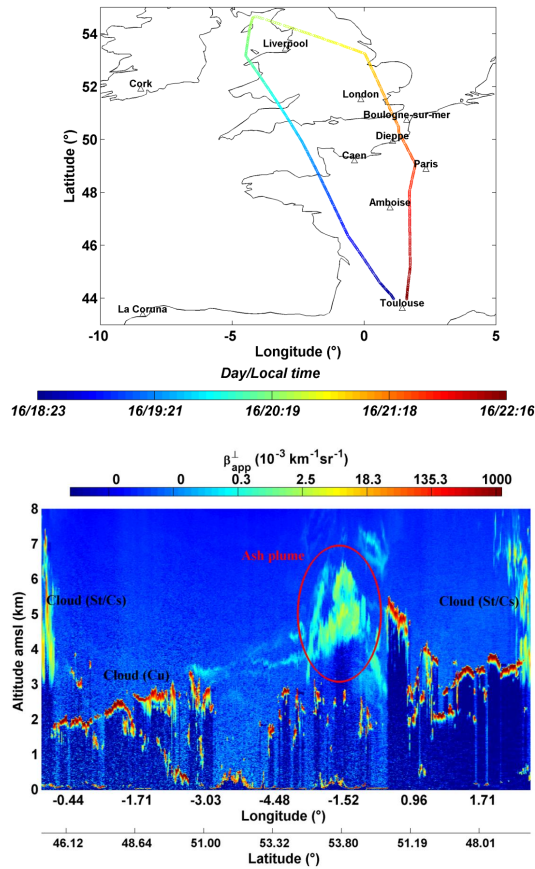


Fig. 6. The same as Fig. 3 for 16 May 2010, above UK.

French airborne lidar measurements for Eyjafjallajökull ash plume survey

P. Chazette et al.

Title Page

Abstract Introduction

Conclusions References

Tables Figures

◀ ▶

◀ ▶

Back Close

Full Screen / Esc

Printer-friendly Version

Interactive Discussion

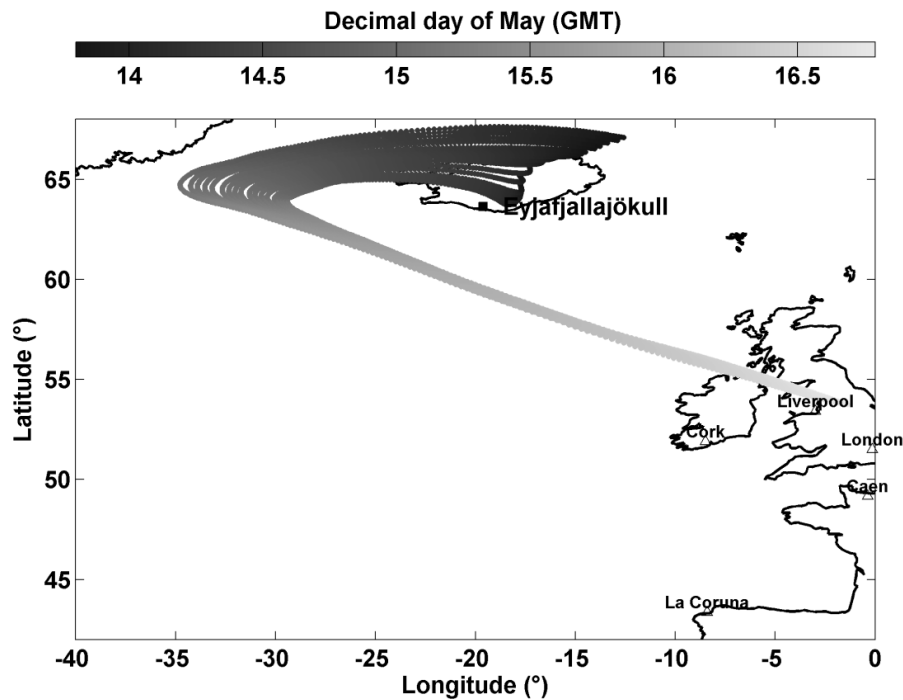


Fig. 7. The same as Fig. 6 for 16 May 2010.

French airborne lidar measurements for Eyjafjallajökull ash plume survey

P. Chazette et al.

Title Page

Abstract Introduction

Conclusions References

Tables Figures

◀ ▶

◀ ▶

Back Close

Full Screen / Esc

Printer-friendly Version

Interactive Discussion



French airborne lidar measurements for Eyjafjallajökull ash plume survey

P. Chazette et al.

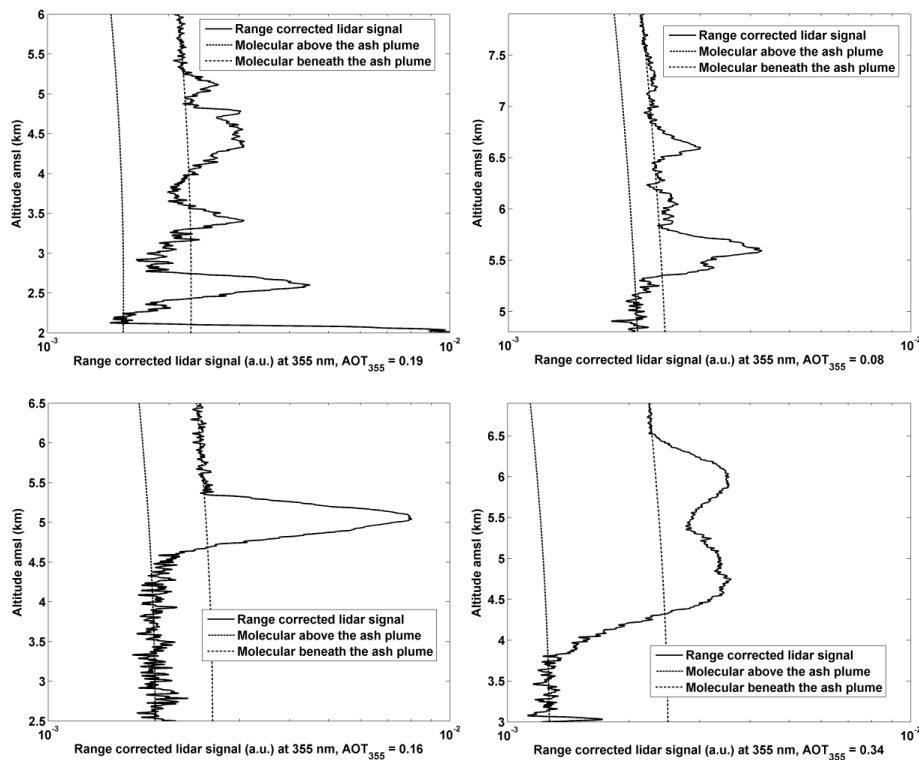


Fig. 8. Range-corrected lidar signal on 12 and 16 May 2010: top-left panel for the plume of 12 May, top-right panel for the plume crown of 12 May, bottom-left panel for the filament of 12 May, and bottom-right panel for the plume of 16 May. The molecular contributions have been simulated for each normalization altitude, and are also given in each figure.

Title Page

Abstract

Introduction

Conclusions

References

Tables

Figures

◀

▶

◀

▶

Back

Close

Full Screen / Esc

Printer-friendly Version

Interactive Discussion

French airborne lidar measurements for Eyjafjallajökull ash plume survey

P. Chazette et al.

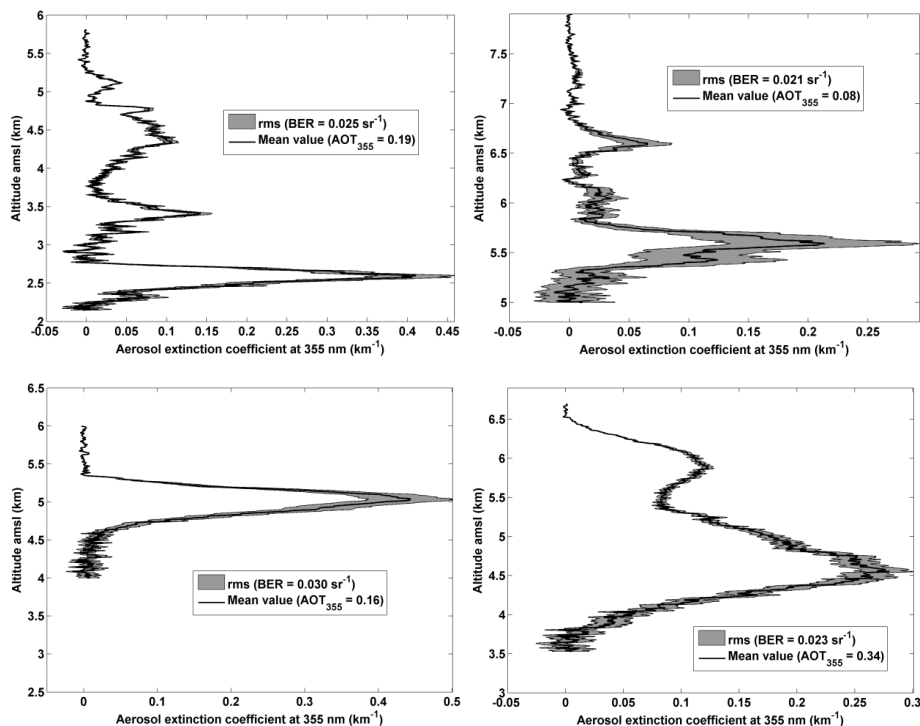


Fig. 9. Mean profiles of the aerosol extinction coefficient on 12 and 16 May 2010: top-left panel for the plume of 12 May, top-right panel for the plume crown of 12 May, bottom-left panel for the filament of 12 May, and bottom-right panel for the plume of 16 May. The standard deviation (rms) linked to the retrieval uncertainty is also given by the gray area. The BER used for the inversion are also indicated.

Title Page

Abstract

Introduction

Conclusions

References

Tables

Figures

◀

▶

◀

▶

Back

Close

Full Screen / Esc

Printer-friendly Version

Interactive Discussion

French airborne lidar measurements for Eyjafjallajökull ash plume survey

P. Chazette et al.

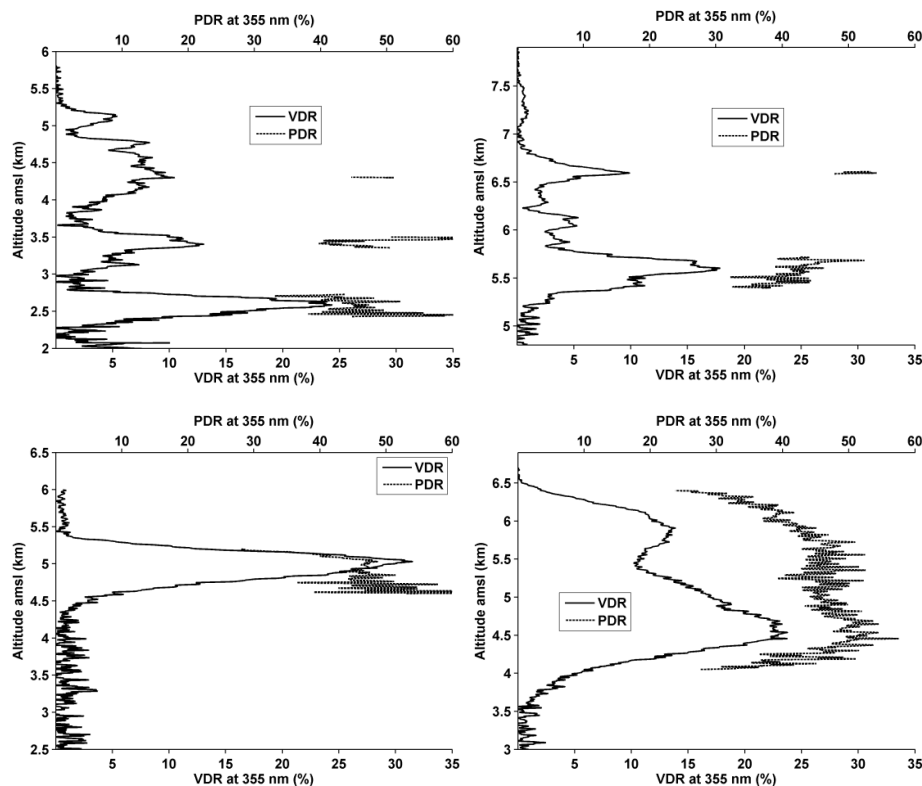


Fig. 10. Mean profiles of both the VDR and the PDR on 12 and 16 May 2010: top-left panel for the plume of 12 May, top-right panel for the plume crown of 12 May, bottom-left panel for the filament of 12 May, and bottom-right panel for the plume of 16 May.

[Title Page](#)[Abstract](#)[Introduction](#)[Conclusions](#)[References](#)[Tables](#)[Figures](#)[◀](#)[▶](#)[◀](#)[▶](#)[Back](#)[Close](#)[Full Screen / Esc](#)[Printer-friendly Version](#)[Interactive Discussion](#)